SimBuild
2024

Eleventh National Conference of IBPSA-USA
Denver, Colorado
May 21 – 23, 2024

ANT: A Multizone Indoor Air Quality (IAQ) and Ventilation Analysis Plug-in for Algorithm Aided Design

Jialei Shen[1,2], W. Stuart Dols[1], and Brian J. Polidoro[1]
[1] National Institute of Standards and Technology (NIST), Gaithersburg, MD, USA
[2] University of Maryland, College Park, MD, USA

Abstract

To facilitate the design and analysis related to indoor air quality (IAQ) and ventilation in buildings, a plug-in named ANT (contam-in-ANT) has been developed for Rhino/Grasshopper, an algorithm aided design platform. ANT is a whole-building IAQ and ventilation analysis tool based on CONTAM. ANT can be utilized to perform multizone simulations to assess airborne transmission risks, estimate health impacts due to inhalation exposure, perform parametric analyses, and optimize performance-driven building design and system settings. Cost-effective optimization of IAQ and ventilation for existing buildings is critical to the retrofitting required for these structures to achieve sustainability goals by 2050. A case study of a medium office building is used to demonstrate ANT and the post-processing of simulation results within Rhino/Grasshopper.

Introduction

Indoor air quality (IAQ) plays a critical role in ensuring the health and wellbeing of individuals within built environments. The spread of respiratory diseases, such as COVID-19, is intricately linked to the effectiveness of ventilation systems in buildings, and thus IAQ (Rayegan et al., 2023; Shen et al., 2021b, 2021a; Yan et al., 2022a, 2022b). With the increasing challenges posed by climate change, including the frequent occurrence of environmental disasters like wildfires, there is a pressing need to evaluate and optimize building ventilation systems to enhance IAQ, which should start at the early phase of building designs (Cheng et al., 2018). IAQ has become increasingly crucial in the context of designing and operating energy-efficient and sustainable buildings while ensuring healthy environments. Balancing the demands of sustainability with health considerations is essential in modern building practices. This is paramount not only for new building designs but also for retrofitting existing structures. Cost-effective optimization of IAQ and ventilation systems is a vital component of retrofitting existing buildings to meet sustainability targets by 2050.

Rhino/Grasshopper [a] is a widely used platforms for algorithm aided architecture design today. Many building performance analysis plug-ins have been developed on the platform, making Rhino/Grasshopper a powerful tool for architects aiming to design high-performance buildings. Some of the most prevalent plug-ins include building energy simulation tools like Honeybee, Dragonfly and Archsim (built on EnergyPlus and OpenStudio), weather data analysis tools such as Ladybug, computational fluid dynamics (CFD) tools for indoor and outdoor airflow modelling such as Butterfly and Eddy (based on OpenFOAM), thermal and daylight building simulation tools like TRNLizard (based on TRNSYS), and building ventilation and infiltration calculation tools like Eabbit-NV and Pigeon (based on CONTAM). Eabbit-NV is a tool calculating natural ventilation rates of buildings with different window configurations (Han, 2022). Pigeon is a plug-in that calculates multizone natural ventilation and infiltration airflows based on CONTAM version 3.2 (Šileryte et al., 2017). However, a notable limitation of both these tools is their inability to simulate mechanical ventilation and contaminant dispersion, which are essential components of built environment analysis. This highlights a significant gap in the availability of tools on Rhino/Grasshopper that are adept at comprehensive IAQ and ventilation analysis, especially concerning indoor air contaminants, occupant exposure, and their health implications. Addressing this gap is imperative to promote healthier built environments.

CONTAM was developed by the National Institute of Standards and Technology (NIST) to accomplish whole-building, multizone IAQ and ventilation analyses (Dols

[a] Certain commercial equipment, instruments, software, or materials, commercial or non-commercial, are identified in this paper in order to specify the experimental procedure adequately. Such identification does not imply recommendation or endorsement of any product or service by NIST, nor does it imply that the materials or equipment identified are necessarily the best available for the purpose.

and Polidoro, 2020). Leveraging detailed physics-based models for air and contaminant mass balance, it ensures accurate and reliable results, all while minimizing simulation costs. Many studies have been conducted to validate its simulations (Fine and Touchie, 2021; Haghighat and Megri, 1996). The software's capabilities have been significantly expanded through the integration of auxiliary tools like CFD0, CONTAM3DExporter, and ContamFactorial (Dols et al., 2020; Wang et al., 2010). These additions extend CONTAM's functionality to include detailed airflow distribution analysis, co-simulation with EnergyPlus and TRNSYS, airborne transmission risk assessment for respiratory diseases, and extensive parametric analysis. As a result, CONTAM has gained widespread adoption among engineers and researchers, becoming a tool of choice for diverse applications (Dols et al., 2021; Justo Alonso et al., 2022; Yan et al., 2022a, 2022b; Yang, Wang, Raftery, et al., 2023).

To facilitate IAQ and ventilation analysis during the architectural design and urban planning processes, we incorporated CONTAM functions into a plug-in to Rhino/Grasshopper. This plug-in named "ANT", inspired by “contaminant” (or "contam-in-ANT"), was developed to bridge the gap between CONTAM and the architectural design platform. The robust 3D geometry modelling and visualization capabilities of Rhino/Grasshopper also provide a different user experience compared to the existing CONTAM user interface (ContamW).

Overview of ANT architecture

ANT was developed using C#, one of the options provided by Rhino/Grasshopper. Multiple dependencies were used to develop the plug-in and to perform CONTAM simulations, including Rhino and Grasshopper software development kits (SDKs) and CONTAM-related application programming interfaces (APIs) and files. The architecture diagram of ANT is shown in Figure 1.

ANT APIs and workflow

The APIs of Rhino and Grasshopper are utilized in the creation of plug-in components and for retrieving data from the Rhino and Grasshopper canvas, such as information on geometry (e.g., volume, surface area, and surface orientation), which is used in creating CONTAM elements (e.g., zone volume, floor area, and airflow leakage paths). The ContamP API (contam-p.dll), developed by NIST, is used for defining the elements of a CONTAM project such as zones, paths, contaminant species, air handling units (AHUs), schedules, filters, and occupancy elements. The API also enables the generation of CONTAM project (PRJ) files based on these defined elements.

The ANT plug-in comes integrated with the latest NIST-developed ContamX executable file (contamx3.exe), which runs simulations for the generated PRJ files and subsequently produces the simulation result (SIM) files.

The ANT plug-in is equipped with two additional executable files. The first, CONTAM_EPWtoWTH.exe, converts EnergyPlus weather (EPW) files into CONTAM weather (WTH) files. The second, simread.exe, reads-in SIM files and exports text files containing selected output parameters which can then be utilized for further post-processing. The results generated from these processes can be seamlessly visualized on the building geometry within Rhino, offering users an intuitive and clear representation of the simulation results.

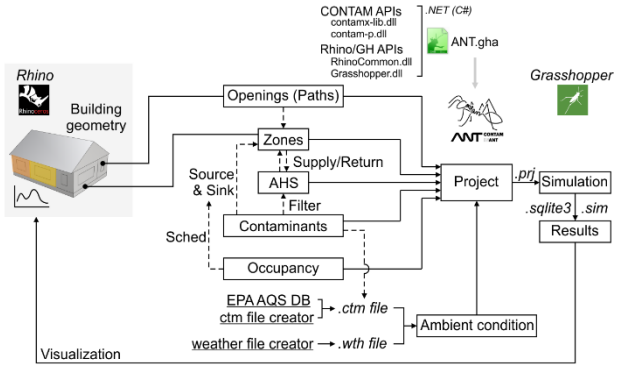

Figure 1 Architecture diagram of ANT.

ANT components

In ANT, 90 distinct components have been developed and organized into 12 sub-categories, encompassing Geometry, HVAC, Filter, Schedule, Species, Source/Sink, Occupancy, Airflow, Library, Ambient, Simulation, and Results (Figure 2). These components were developed based on the elements used in CONTAM. Descriptions of each sub-category are presented in Table 1.

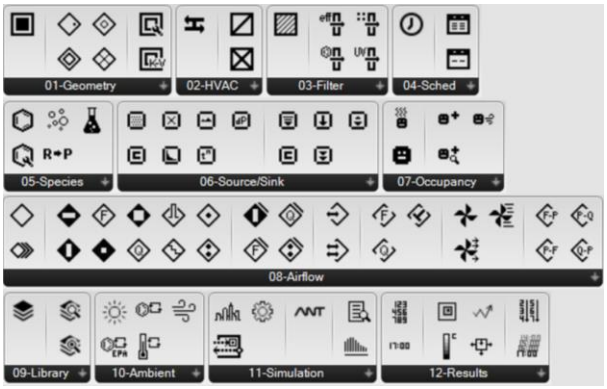

Figure 2 ANT components.

Table 1 ANT sub-categories.

No.	Sub-category	Description
1	Geometry	Read geometries from Rhino to generate zone and surface elements (e.g., window, door)
2	HVAC	Define simple air handling units (AHUs), supplies, and returns
3	Filter	Define filter elements: constant efficiency, simple gaseous, simple particle, and ultraviolet germicidal irradiation (UVGI)
4	Schedule	Define day and week schedules for dimensionless variables, temperature, and occupancy
5	Species	Define contaminant species and kinetic reactions; Contains a particle distribution calculator
6	Source/Sink	Define source and sink elements for specified contaminants
7	Occupancy	Define occupant emission, exposure, and health impacts
8	Airflow	Define different types of airflow elements and create airflow paths associated with airflow elements
9	Library	Create/read CONTAM species, filter, day schedule, and wind profile libraries
10	Ambient	Define ambient conditions for simulations: weather and contaminants; Customize wind profiles; Generate weather (WTH) and contaminant (CTM) files
11	Simulation	Generate CONTAM project (PRJ) files with specified simulation parameters and inputs from other components and run simulations
12	Results	Read and visualize simulation results (SIM)

ANT applications

ANT can be used to simulate building infiltration, natural ventilation driven by indoor/outdoor pressure and temperature difference, mechanical ventilation by AHUs or airflow paths associated with fan flow elements, indoor contaminant emissions, inter-zone transfer and decay of indoor contaminants, kinetic reactions, contaminant filtration by AHUs or standalone air cleaners, occupant emission and exposure to contaminants, risk, and health assessment. In combination with optimization plug-ins on Grasshopper, such as *Octopus* (Vierlinger, 2018), ANT can be used for optimizing building design and system settings.

ANT can handle multiple projects simultaneously, enabling IAQ analyses across buildings, communities, or even entire cities. This feature is crucial for tracking human exposure in different building scenarios, offering vital insights for estimating the transmission of respiratory diseases across populations, a task intricately linked to human mobility trajectory and behavior.

ANT goes beyond the simulation outputs of CONTAM, providing human exposure and health-related analyses. It calculates exposure based on defined human mobility trajectory, behaviors, respiratory activities, and the use of personal protective equipment (PPE) such as face masks. The potential health impacts of exposure are quantified through the estimation of disability-adjusted life years (DALYs), i.e., the sum of the years of life lost to due to premature mortality (YLLs) and the years lived with a disability (YLDs) due to prevalent cases of the disease or health condition in a population (Huijbregts et al. 2005; WHO 2020). Using DALYs for a regulated and quantitative assessment of health outcomes due to indoor air contaminant exposure offers a method to estimate the healthcare costs related to health loss. This approach provides a crucial metric to assess the economic impact of air quality on public health. Additionally, it enables the execution of cost-effectiveness analyses for upgrading buildings or systems to improve IAQ, providing a foundational basis for informed decision-making in environmental health policy and building management. For some air contaminants like ozone, DALYs can be estimated through Equation (1) (Logue et al., 2012).

$$DALYs = [(\partial DALY/\partial intake)_{cancer} \times ADAF + (\partial DALY/\partial intake)_{non\text{-}cancer}] \times intake \quad (1)$$

where $(\partial DALY/\partial intake)_{cancer}$ and $(\partial DALY/\partial intake)_{non\text{-}cancer}$ are DALYs lost per unit of intake from cancer and non-cancer effects (years/kg). *ADAF* is the age-dependent adjustment factor. In this study, we assumed an *ADAF* of 1.6, which is approximately the average across all populations (Shen, 2023). The variable *intake*

represents the total intake of the pollutant (i.e., accumulated pollutant inhalation in this study). For scenarios involving infectious respiratory diseases like COVID-19, ANT enables the simulation of airborne particle transmission within multizone environments and the calculation of infection probabilities, based on inhaled doses of viral particles, via the Wells-Riley model (Albettar et al., 2022a, 2022b; Shen et al., 2021b, 2021a; Sze To and Chao, 2010; Yan et al., 2022a, 2022b; Yang, Wang, Raftery, et al., 2023).

ANT takes advantage of integration with Rhino/Grasshopper by projecting CONTAM results directly onto the building geometry. Additionally, it allows users to plot temporal data over selected time periods within Rhino. Users can also view animated representations of concentration changes over user-specified time periods.

ANT includes a component of the CONTAM particle distribution calculator (Dols and Polidoro, 2014), facilitating the creation of realistic particle size distributions for CONTAM simulations. Furthermore, ANT connects to the U.S. EPA Air Quality System (AQS) database, allowing for the generation of CONTAM-specific, ambient contaminant (CTM) files for typical atmospheric contaminants in U.S. cities, such as PM2.5, ozone, NO_2, and SO_2 (U.S. EPA, 2023). ANT also excels in parametric analyses, addressing variables that are challenging to specify directly, such as human respiratory rates and activities. It enables Monte Carlo simulations in IAQ analysis within Grasshopper, paving the way for a more representative and accurate simulation output.

In summary, ANT has the capability to conduct multizone IAQ and ventilation analyses to assess airborne transmission risks, estimate health impacts due to inhalation exposure, perform parametric analyses, and optimize performance-driven building design and system settings. Its scope can extend from a single building to community or city scales, facilitating IAQ and occupant exposure analyses at these broader levels considering the significance of urban-scale IAQ and health analysis (Katal et al., 2019, 2021; Mortezazadeh et al., 2022; Yang, Wang, Stathopoulos, et al., 2023), and thus contributing to healthier living and working environments. ANT can be accessed at https://www.food4rhino.com/en/app/ANT.

Case study

The U.S. Department of Energy (DOE) Medium Office Building was used to demonstrate the capabilities of ANT. Pertinent details of the building are presented below. For more details, see Ng et al., 2012, 2019. It should be noted that CONTAM itself has been validated in previous studies available within the literature.

Geometry

The Medium Office is a three-story building that has a footprint of approximately 1 662 m^2 (49.9 m × 33.3 m) and a total floor area of about 4 985 m^2. The floor-to-ceiling height is 2.74 m and the floor-to-floor height is 4.0 m including the height of a return air plenum above each floor. Each level has the same floor plan – four perimeter zones and a core zone (Figure 3). In the CONTAM model, a restroom with a footprint of 10 m × 10 m was carved out of the core zone. The CONTAM model also has a 3 m × 10 m stairwell and a 3 m × 10 m elevator shaft that both span all levels of the building and serve to account for an area within the building that may have significant buoyancy-driven airflows (Figure 3).

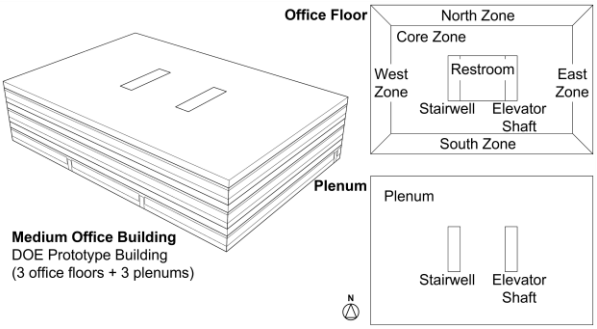

Figure 3 Schematic of the Medium Office Building.

Airflow paths

The interior leakage between occupied zones was defined as 5.27 cm^2/m^2 at 4 Pa at the mid-height of each interior surface. The exterior wall leakage, as well as shaft and stairwell walls, was divided into three equal sections by height above the floor to account for any potential thermal stack effect. Each wall section had a leakage of 5.27 cm^2/m^2 at 4 Pa. The roof leakage was also assumed to be 5.27 cm^2/m^2 at 4 Pa and was modelled using a single leakage path. Exterior windows (fixed, window-wall ratio of 0.5) were modelled using the two-way opening model. Exterior doors (6 on Floor 1) were modelled using the two-way opening with an orifice model to simulate the 2.5 cm undercut of each door. Return grilles were modelled at the ceiling of each zone assuming an orifice of 1 m^2, connecting each office space with the plenum. Between the restroom and core zones, a 0.186 m^2 transfer grille (orifice) was modelled. Exterior surfaces were simulated assuming a wind pressure profile designated for low-rise walls (Ng et al., 2019).

Air handling systems

The air handling systems were modelled in ANT as constant air volume (CAV) systems. The design supply air flow rates were: Core Zones 12 492 m^3/h, North and

South Zones 2 860 m^3/h each, and East and West Zones 2 288 m^3/h each. A single return for each AHU was set to 90 % of the total supply airflow rate of all the zones served. MERV 11 filters were used in the systems. Each restroom included an exhaust-only AHU with a design flow rate of 360 m^3/h.

Occupancy

The occupancy number and schedule were defined based on the settings from the DOE prototype model. The peak occupancy of each zone was as follows: Core Zone 41.1 persons, South and North Zones 9.41 persons each, and East and West Zones 7.53 persons each. All other zones were presumed to be unoccupied. Occupants in zones were scheduled according to Figure 4. The building was unoccupied on Sundays and holidays.

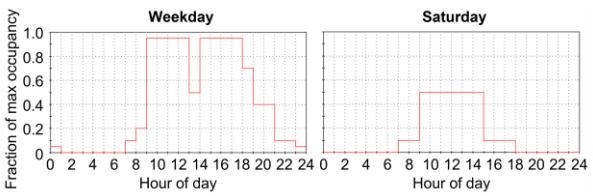

Figure 4 Occupancy schedule.

Contaminant and weather settings

Three air contaminants were simulated for demonstration, i.e., carbon dioxide (CO_2), ozone, and infectious aerosols for a generic pathogen.

Indoor CO_2 concentration was dependent on the outdoor concentration, the number of occupants within a zone, and the outdoor air ventilation rate of the zone. In this example, it was assumed that each person generated 0.018 m^3 CO_2 per hour (Sakamoto et al., 2022), and the ambient CO_2 concentration was 400 ppm_v[b].

Ozone is a highly reactive compound that can affect IAQ and human health (Carter et al., 2023; Link et al., 2023; Shen and Gao, 2018; Xu et al., 2023). While ozone can originate indoors, it is mainly from outdoors and can enter the building through ventilation or infiltration. For this case, ambient ozone concentrations, obtained from the EPA AQS database (the River Terrace site in Washington DC, the year 2017), were provided to the simulation via a CTM file, and a constant ozone removal sink was simulated having a deposition velocity of 14.8 m/h for each interior surface (Shen and Gao, 2018; Yao and Zhao, 2018).

Infectious aerosols are exhaled by infected individuals and are directly related to the airborne transmission and risk of infection of respiratory diseases (Shen et al., 2021a; Yan et al., 2022b). In this study, a generic infectious virus (IV1) contaminant was modelled assuming a particle diameter of 1 µm and a generation rate of 100 quanta/h (#/h) (Shen et al., 2021b, 2021a). It was assumed that there is only one asymptomatic infector in this building, who was present every weekday of the simulation according to the schedule shown in Table 2. The AHUs, except for the exhaust-only AHU for each restroom, were modelled to filter IV1 in the supply air at a removal efficiency of 50 %. Weather data for Ronald Reagan Washington National Airport was utilized.

Table 2 Weekday infector schedule.

Time	Zone
0 – 9	Not in the building
9 – 12	Core Zone, Floor 1
12 – 13	West Zone, Floor 1
13 – 18	Core Zone, Floor 1
18 – 24	Not in the building

Simulation results

Transient simulations were performed for one week (Sunday January 1 to Saturday January 7) with a time step of 5 min.

Indoor contaminant distribution

ANT provides color-scaled visualization of contaminant concentrations for each zone and time step. Figure 5 shows concentration in across the entire building and specifically for the zones on Floor 1 for 12:00 Monday January 2.

Figure 6 shows the CO_2 concentration during the one-week simulation period in the Core Zones of each floor, revealing the cyclical nature of CO_2 as the occupancy rises and falls each day. Animation of contaminant concentration over time is also made possible with ANT. Screenshots between 17:00 and 24:00 on January 2 are shown in Figure 7 for CO_2 concentration. The CO_2 concentration begins to decay after the occupants have left at 18:00. Animation can help to illustrate the complex transport behavior associated with ventilation system flows and stack effect.

[b] In this work, CO2 concentrations are expressed in ppm_v, which is equivalent to µL/L. Ozone levels are expressed in ppb_v, which is equivalent to nL/L.

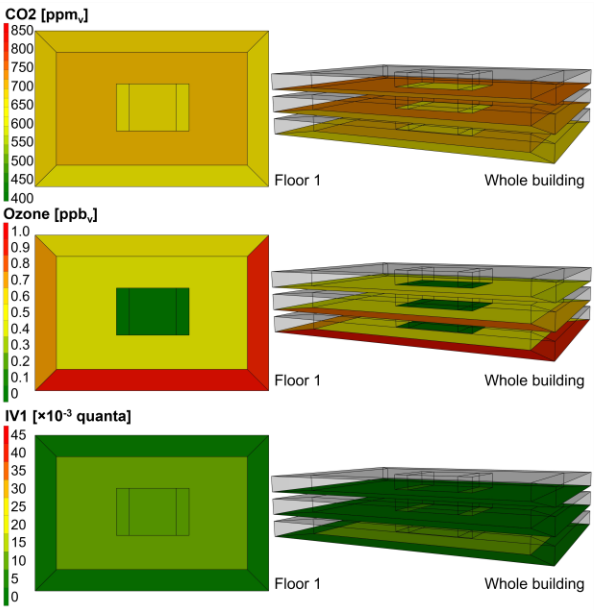

Figure 5 Distribution of CO_2, ozone, and IV1 in Medium Office Building at 12:00 January 2.

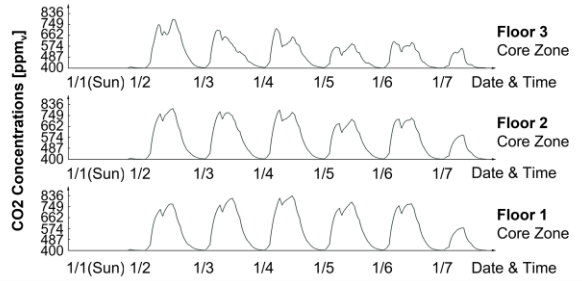

Figure 6 CO_2 concentration in the Core Zones of each floor.

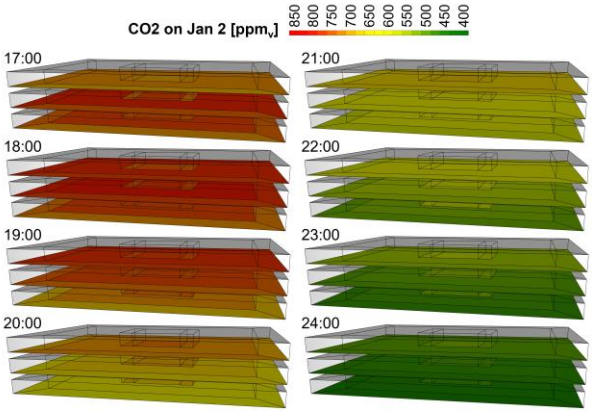

Figure 7 CO_2 concentration change on January 2 between 17:00 and 24:00.

Ozone exposure and DALY assessment

The accumulated ozone exposure of the occupant, with the schedule in Table 2, during the simulation period was 1.76×10^{-6} kg. To estimate the DALYs due to the long-term exposure to ozone, a year-long simulation of ozone exposure was performed, resulting in an annual exposure of 1.13×10^{-4} kg to ozone. This is equivalent to 16.6 years of DALYs per 100,000 population per year with a ∂DALY/∂intake factor of 0.92 year/kg (Huijbregts et al., 2005).

IV1 infection probability and mitigation

Infection probability was calculated using the Wells-Riley model based on exposure to IV1 on weekdays. It was assumed that the virus particles remained infectious as long as they were airborne. The exposure scenarios simulated and the resulting infection probability were: (1) Assuming the schedule of the receptor being the same as the infector (Table 2), an infection probability of 16.3 %; (2) Assuming the receptor occupied the Core Zone on Floor 2 during working hours and never occupied the same zones as the infector, an infection probability of 2.6 %. The latter scenario demonstrates that virus-laden aerosols may still be transported between building floors and zones.

One approach to mitigate infection risk is to introduce more outdoor air into the building. For the previous scenario (1), raising the outdoor air fraction (OAF) of the AHU from 0.1 to 0.5 reduced the infection probability from 16.3 % to 13.5 %, and increasing the outdoor air fraction to 1.0 further reduced it to 11.4 % (Table 3).

Face masks have been used as another approach to mitigate exposure to airborne pathogens. For the previous scenario (1), assuming the receptor was wearing a mask with a protection efficiency of 50 % the infection probability was reduced to 8.5 %, 75 % protection efficiency reduced it to 4.4 %, and a protection efficiency of 95 % reduced the infection probability to 0.9 %. These assumptions show that wearing a mask, even a less efficient one, could effectively reduce infection probability.

Table 3 Effectiveness of mitigation strategies where infector and receptor occupied same zones.

Strategy	**Infection probability [%]**	**Relative change from Base [%]**
OAF=0.1, no mask (Base case)	16.3	
OAF=0.5, no mask	13.5	17.2 ↓
OAF=1.0, no mask	11.4	30.1 ↓
OAF=0.1, mask=50 %	8.5	47.9 ↓
OAF=0.1, mask=75 %	4.4	73.0 ↓
OAF=0.1, mask=95 %	0.9	94.5 ↓

Parametric analysis

Various plug-ins and features of Grasshopper were leveraged to perform a parametric analysis to demonstrate the use of ANT to show the impacts of the variation of quanta generation rates on infection probability. A list of stochastic values in a normal distribution was utilized as the quanta generation rate, with a mean value of 100 quanta/h and a standard deviation of 25 quanta/h. The calculated infection probability was 16.3 % ± 3.8 % for the base case in Table 3.

Performance-driven optimization

Performance-driven optimization of building design and system settings can be performed by utilizing plug-ins in Grasshopper. Multi-objective optimization is usually conducted to find the optimal setting for multiple objectives and has been widely used in building research areas (Baba et al., 2023). Increasing the OAF of an AHU would reduce the infection probability. However, it would also increase the indoor concentration of ozone when outdoor air has a higher level of ozone than the indoors. To find the optimal OAF that balances ozone exposure and infection probability, a multi-objective optimization with genetic algorithms was applied using the *Octopus* plug-in.

Figure 8 shows results of 461 simulations in total varying OAF between 0 and 1. The datapoints on the Pareto front represent the optimal OAFs of the studied scenario. The selection depends on the weight of each objective, i.e., ozone exposure and infection probability. If we assume that the infection probability needs to be maintained below 12 % while no specific control target for indoor ozone, the optimal OAF to be 0.83, resulting in an ozone exposure of 1.788×10^{-6} kg.

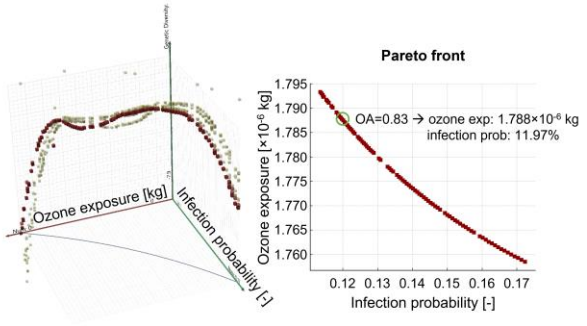

Figure 8 Multi-objective optimization results.

Community-scale IAQ analysis

ANT can generate multiple projects and perform simulations simultaneously, which makes it possible to conduct IAQ analysis for a community with multiple buildings or even a city. People are usually exposed to various species and concentration levels in different scenarios, depending on building settings, human behavior, and mobility trajectory.

In this study, a simple community example was established, which included the Medium Office Building and a single-family house (Figure 9). A DOE prototype residential building was used as the single-family house, which consisted of two floors and an attic, as well as fixed windows on exterior walls. Each floor was defined as a single zone. The wall and roof leakage and pollutant characteristics of the office building were also assigned to the house. To simplify the demonstration, no AHU was modelled in the house. To track personal exposures, an individual who lives and works in this simplified community was defined. The individual's schedule in the office building was defined in Table 2. Before and after work, the individual commutes one hour between the house and the office (8 a.m. to 9 a.m. to work, and 6 p.m. to 7 p.m. back home). It is assumed that the individual spends all other hours at the house on Floor 1. During commuting, it is assumed that the individual is exposed to the ambient contaminant levels. No indoor ozone generation was assumed in either the office or home.

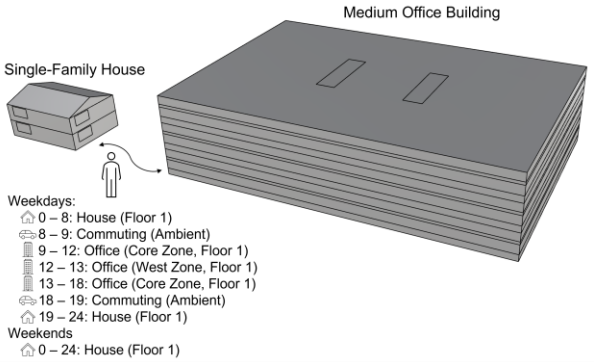

Figure 9 A simple community example with the Medium Office Building and a single-family house, and an individual who lives and works in this community.

Figure 10 shows the distribution of ozone concentration in the house and the office building at 12:00 on January 2. Considering the individual's mobility trajectory, the ozone exposure over time is shown in Figure 11. The individual is exposed to the highest level of ozone during commuting (ambient ozone concentration). Considering the human mobility trajectory, the commuting exposure accounted for 67.5 % of the total ozone exposure, whereas the exposure at home accounted for 30.2 % and the exposure in the office 2.3 %. The individual had the highest exposure commuting even though they only spent 8 % (2 h) of their weekday commuting. Studies

like these can help to understand the contribution of each scenario or behavior to the exposure to a certain contaminant.

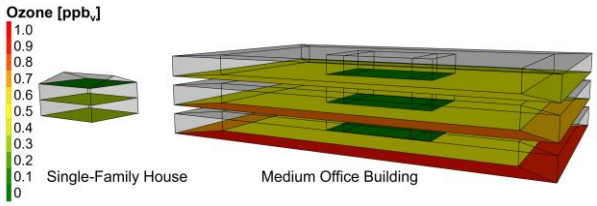

Figure 10 Distribution of ozone concentration in the house and the office at 12:00 January 2.

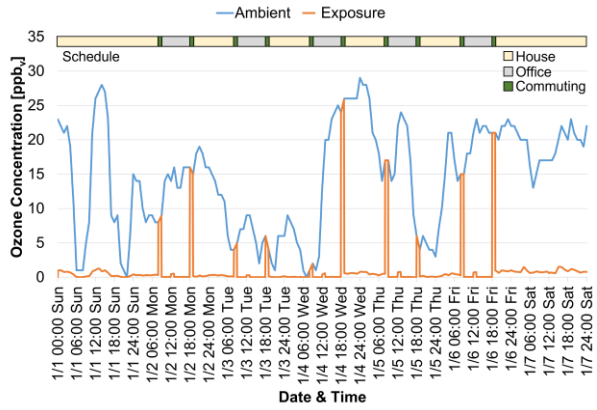

Figure 11 The individual's exposure to ozone based on the mobility trajectory.

Conclusion

ANT is a whole-building IAQ and ventilation analysis plug-in for Rhino/Grasshopper that is based on, but also extends, the capabilities of CONTAM. It was developed to meet the increasing demand for buildings with high performance associated with IAQ and health. ANT has the capability to conduct multizone IAQ and ventilation analyses, assess airborne transmission, estimate health impacts associated with inhalation exposure, perform parametric analyses, and optimize performance-driven building design and system settings. The case study illustrated the process of running ANT for a medium office building and a simplified community that consists of two buildings, and demonstrated post-processing capabilities of simulation results.

The emphases on IAQ and health considerations during building design or retrofit are not only significant for human health, but also important for sustainability and environmental justice. Cost-effective optimization of IAQ and ventilation for existing buildings is critical to the retrofitting required for these structures to achieve sustainability goals by 2050. It is essential to acknowledge that the real-world application of building and system design involves more complex factors beyond just IAQ and health considerations. For example, when designing and operating a healing environment in a hospital, it is necessary to account for a range of aspects that impact patient stress and healing quality. These factors can sometimes conflict with the principles of designing conventional ventilation systems. As such, it is crucial to adopt a holistic approach, taking into account the diverse factors of built environments to effectively address real-world challenges.

Future work

To allow detailed airflow within and surrounding buildings, CFD simulations can be integrated into the ANT plug-in. The integration of existing CFD plug-ins on Grasshopper with ANT will be explored in the future.

The building model presented in this paper is a basic prototype, characterized by idealized layouts and settings. For a more comprehensive understanding, future research should explore a wider variety of building scenarios. The cost-effective (Höfler et al., 2017) optimization of ventilation strategies towards a better IAQ on existing buildings' deep renovation will be explored to ensure reliability, applicability and facilitated validation of good ventilation practices. Additionally, the validation process for these example cases will be undertaken to ensure their reliability and applicability.

The present work presented a very simple community example with two buildings and simple human mobility trajectory and behavior. More complicated community examples or even city-scale examples with more complex and realistic building and human settings will be explored.

Other potential future work is collaborating with energy simulation tools, such as Honeybee on Grasshopper, or EnergyPlus itself, to perform coupling simulation between IAQ and energy performance on Rhino/Grasshopper.

In the future, we will also explore the integration of control algorithms, especially intelligent controls, into IAQ analyses conducted by ANT.

References

Albettar, M., L. (Leon) Wang, and A. Katal. 2022b. A real-time web tool for monitoring and mitigating indoor airborne COVID-19 transmission risks at city scale. *Sustainable Cities and Society*, *80*:103810.

Baba, F. M., H. Ge, R. Zmeureanu, and L. (Leon) Wang. 2023. Optimizing overheating, lighting, and heating energy performances in Canadian school for climate

change adaptation: Sensitivity analysis and multi-objective optimization methodology. *Building and Environment*, *237*:110336.

Carter, T. J., D. G. Poppendieck, D. Shaw, and N. Carslaw. 2023. A Modelling Study of Indoor Air Chemistry: The Surface Interactions of Ozone and Hydrogen Peroxide. *Atmospheric Environment*, *297*:119598.

Cheng, J., D. Qi, A. Katal, L. (Leon) Wang, and T. Stathopoulos. 2018. Evaluating wind-driven natural ventilation potential for early building design. *Journal of Wind Engineering and Industrial Aerodynamics*, *182*:160–169.

Dols, W. S., C. W. Milando, L. Ng, S. J. Emmerich, and J. Teo. 2021. On the Benefits of Whole-building IAQ, Ventilation, Infiltration, and Energy Analysis Using Co-simulation between CONTAM and EnergyPlus. *Journal of Physics: Conference Series*, *2069*(1):012183.

Dols, W. S., and B. J. Polidoro. 2020. *CONTAM User Guide and Program Documentation Version 3.4*.

Dols, W. S., B. J. Polidoro, D. Poppendieck, and S. J. Emmerich. 2020. A tool to model the Fate and Transport of Indoor Microbiological Aerosols (FaTIMA).

Dols, W. S., B. J. Polidoro. 2014. CONTAM Particle Distribution Calculator | NIST.

Fine, J. P., and Touchie, M. F. 2021. Evaluating ventilation system retrofits for high-rise residential buildings using a CONTAM model. *Building and Environment, 205*: 108292.

Haghighat, F., and Megri, A. C. 1996. A Comprehensive Validation of Two Airflow Models - COMIS and CONTAM. *Indoor Air, 6(4)*: 278-288.

Han, E. J. 2022. Eabbit - Natural Ventilation Tool | Food4Rhino.

Höfler, K., Maydl, J., Venus, D., Sedlák, J., Struhala, K., de Almeida, M. G., Ferreira, M. A. P. S., Brito, N., Baptista, N., and Fragoso, R. 2017. Shining Examples of Cost-Effective Energy and Carbon Emissions Optimization in Building Renovation. *Annex 56 (2nd Edition)*: 154.

Huijbregts, M. A. J., L. J. A. Rombouts, A. M. Ragas, and D. van de Meent. 2005. Human-toxicological effect and damage factors of carcinogenic and noncarcinogenic chemicals for life cycle impact assessment. *Integrated Environmental Assessment and Management, 1*(3):181–244.

Justo Alonso, M., W. S. Dols, and H. M. Mathisen. 2022. Using Co-simulation between EnergyPlus and CONTAM to evaluate recirculation-based, demand-controlled ventilation strategies in an office building. *Building and Environment*, *211*:108737.

Katal, A., M. Albettar, and L. (Leon) Wang. 2021. City Reduced Probability of Infection (CityRPI) for Indoor Airborne Transmission of SARS-CoV-2 and Urban Building Energy Impacts. *MedRxiv*, 2021.01.19.21250046.

Katal, A., M. Mortezazadeh, and L. (Leon) Wang. 2019. Modeling building resilience against extreme weather by integrated CityFFD and CityBEM simulations. *Applied Energy*, *250*:1402–1417.

Link, M. F., A. Shore, B. H. Hamadani, and D. Poppendieck. 2023. Ozone Generation from a Germicidal Ultraviolet Lamp with Peak Emission at 222 nm. *Environmental Science and Technology Letters*, *10*(8):675–679.

Logue, J. M., Price, P. N., Sherman, M. H., and Singer, B. C. 2012. A Method to Estimate the Chronic Health Impact of Air Pollutants in U.S. Residences. *Environmental Health Perspectives, 120*(2): 216.

Mortezazadeh, M., L. L. Wang, M. Albettar, and S. Yang. 2022. CityFFD – City fast fluid dynamics for urban microclimate simulations on graphics processing units. *Urban Climate*, *41*:101063.

Ng, L. C., A. Musser, A. K. Persily, and S. J. Emmerich. 2012. Indoor air quality analyses of commercial reference buildings. *Building and Environment*, *58*:179–187.

Ng, L. C., A. Musser, A. K. Persily, and S. J. Emmerich. 2019. *Airflow and Indoor Air Quality Models of DOE Prototype Commercial Buildings*.

Rayegan, S., C. Shu, J. Berquist, J. Jeon, L. (Grace) Zhou, L. (Leon) Wang, H. Mbareche, P. Tardif, and H. Ge. 2023. A review on indoor airborne transmission of COVID-19– modelling and mitigation approaches. *Journal of Building Engineering*, *64*:105599.

Rutten, D. 2021. Galapagos Optimization.

Sakamoto, M., Li, M., Kuga, K., Ito, K., Bekö, G., Williams, J., and Wargocki, P. 2022. CO2 emission rates from sedentary subjects under controlled laboratory conditions. *Building and Environment, 211: 108735*.

Shen, J., and Z. Gao. 2018. Ozone removal on building material surface: A literature review. *Building and Environment, 134*:205–217.

Shen, J., M. Kong, B. Dong, M. J. Birnkrant, and J. Zhang. 2021a. A systematic approach to estimating the effectiveness of multi-scale IAQ strategies for reducing the risk of airborne infection of SARS-CoV-2. *Building and Environment*, 107926.

Shen, J., M. Kong, B. Dong, M. J. Birnkrant, and J. Zhang. 2021b. Airborne transmission of SARS-CoV-2 in indoor environments: A comprehensive review. *Science and Technology for the Built Environment*, 1–60.

Shen, J. 2023. Green Design Studio: A Modular-Based Approach for High-Performance Building Design. In Syracuse University.

Šileryte, R., A. D'Aquilio, M. Turrin, and E. van den Ham. 2017. Pigeon | Food4Rhino.

Sze To, G. N., and C. Y. H. Chao. 2010, February. Review and comparison between the Wells-Riley and dose-response approaches to risk assessment of infectious respiratory diseases. *Indoor Air*. Wiley-Blackwell.

U.S. EPA. 2023. AQS API | AirData | US EPA.

Vierlinger, R. 2018. Octopus | Food4Rhino.

Wang, L., W. S. Dols, and Q. Chen. 2010. Using CFD Capabilities of CONTAM 3.0 for Simulating Airflow and Contaminant Transport in and around Buildings. *HVAC&R Research*, *16*(6):749–763.

WHO. 2020. Global Health Estimates: Leading Causes of DALYs.

Xu, F., J. Shen, and Z. Gao. 2023. A field measurement study of the effects of outdoor pollutants and room volumes on indoor fine particle and ozone concentrations. *Journal of Building Engineering*, *78*:107615.

Yan, S., L. Wang, M. J. Birnkrant, Z. Zhai, and S. L. Miller. 2022a. Multizone Modeling of Airborne SARS-CoV-2 Quanta Transmission and Infection Mitigation Strategies in Office, Hotel, Retail, and School Buildings. *Buildings 2023, Vol. 13, Page 102*, *13*(1):102.

Yan, S., L. (Leon) Wang, M. J. Birnkrant, J. Zhai, and S. L. Miller. 2022b. Evaluating SARS-CoV-2 airborne quanta transmission and exposure risk in a mechanically ventilated multizone office building. *Building and Environment*, *219*:109184.

Yang, S., L. (Leon) Wang, P. Raftery, M. Ivanovich, C. Taber, W. P. Bahnfleth, P. Wargocki, J. Pantelic, J. Zou, M. Mortezazadeh, C. Shu, R. Wang, and S. Arnold. 2023. Comparing airborne infectious aerosol exposures in sparsely occupied large spaces utilizing large-diameter ceiling fans. *Building and Environment*, *231*:110022.

Yang, S., L. (Leon) Wang, T. Stathopoulos, and A. M. Marey. 2023. Urban microclimate and its impact on built environment – A review. *Building and Environment*, *238*:110334.

Yao, M., and B. Zhao. 2018. Surface removal rate of ozone in residences in China. *Building and Environment*, *142*(June):101–106.